A combined shape control procedure of cable mesh reflector antennas with optimality criterion and integrated structural electromagnetic concept

Shuxin Zhang[1] · Jingli Du[1] · Dongwu Yang[1] · Yiqun Zhang[1] · Shen Li[1]

Abstract A combined shape control procedure with optimality criterion and integrated structural electromagnetic concept for cable mesh reflector antennas is presented in this study. Using the optimality criterion, the shape control algorithm drives the distorted surface towards the ideal shape. The optimality criterion is implemented by pseudo inverse of sensitivity matrix of surface nodal displacements with respect to cable member dimensions to accelerate the iterative convergence. The following integrated structural electromagnetic design is performed to make good electromagnetic performance by a sequential quadratic programming optimization model. A distorted offset cable mesh reflector antenna is employed to show its effectiveness.

Keywords Shape control · Optimality criterion · Integrated structural electromagnetic · Cable mesh reflector antennas

1 Introduction

As one piece of the most important equipment in space structures, deployable antennas have gained much more attention for space applications. Among the various deployable antennas, cable mesh reflector antennas attract much more interests because they are lightweight, small in size before deployment and have good electromagnetic performance (Miura and Rahmat-Samii 2007). With increasing operating frequencies, the effects of surface error on electromagnetic performance become more severe and the serious requirements on surface accuracy become demanding (Hoferer and Rahmat-Samii 2002). As a key issue, shape control of reflector surface which is proposed to correct the distorted surface is of much importance to satisfy the required surface accuracy (Hafkta and Adelman 1985 R1).

The shape control concept was presented by Haftka and Adelman (1985 R1, R2) in 1985 from simple structural disciplinary for space reflectors, which has brought out a series of analytical and experimental studies in shape control, such as the studies for truss antennas (Haftka and Adelman 1987; Haftka 1991; Mitsugi et al. 1990), cable mesh antennas (Du et al. 2013; Shimizu 1996; Tabata et al. 1992; Tanaka and Natori 2004, 2006), and space membrane antennas (Hill et al. 2013; Jenkins et al. 1999). In 1989, another multidisciplinary concept of integrated structural electromagnetic shape control (Padula et al. 1989) was proposed to overcome the drawback of simple structural shape control. The integrated concept described a direct optimization model with far-field electromagnetic performance rather than implicit limits on surface accuracy. The results (Padula et al. 1989) showed that the integrated structural electromagnetic shape control could obtain better electromagnetic performance comparing with simply reducing surface accuracy, and the integrated procedure was preferred in antenna structural design. The integrated structural electromagnetic concept was also adopted in antenna structural design with satisfactory results (Adelman and Padula 1986; Liu and Hollaway 1998; Tolson and Huang 1992). Later in 2015, the integrated structural electromagnetic shape control was further investigated for cable mesh reflector antennas with approximation method and sensitivity analysis of electromagnetic performance with respect to structural inputs (Zhang et al. 2015).

✉ Jingli Du
jldu@mail.xidian.edu.cn

1 Key Laboratory of Electronic Equipment Structure Design (Ministry of Education), Xidian University, Xi'an, Shaanxi 710071, China

Although the integrated shape control in Zhang et al. (2015) provided better electromagnetic performance than the procedure from simply reducing surface accuracy, it costs much more iterations and more computation time. In 1989, the integrated shape control concept could accelerate the optimization iteration by dropping surface rms error as a constraint instead of eliminating it to provide an effective way of leading to faster convergence. This enlightens us to accelerate the optimization by several iterations from simple structural disciplinary. While the acceleration by introducing structural surface rms error into constraints has already been adopted in Padula et al. (1989), this study presents another way to promote the convergence. It is a common knowledge that the best electromagnetic performance exits when the reflector surface is in the neighborhood of nominal ideal state, or even exactly the nominal ideal state for solid smooth reflectors. This is the optimality criterion which will be employed in the following implementation. A rational criterion method called guide-weight criterion method (Chen and Ye 1986) was proposed and employed in antenna structural design early in 1986.

In this study, the optimality criterion is employed and incorporated in shape control procedure to drive the distorted surface towards the ideal shape, and then integrated structural electromagnetic concept is adopted following the prior optimality criterion. The optimality criterion is implemented by pseudo inverse of sensitivity matrix of surface nodal displacements with respect to cable member dimensions, and the integrated concept is implemented by solving a sequential quadratic programming optimization model with computation of gradient vector and Hessian matrix of electromagnetic performance with respect to cable member dimensions. This combined shape control procedure with optimality criterion and integrated structural electromagnetic concept will provide good electromagnetic performance with faster convergence.

The paper is organized as follows: Section 2 presents the combined shape control algorithm with pseudo inverse formulation and a step length optimization, including the integrated structural electromagnetic procedure. In Section 3, a distorted offset cable mesh reflector antenna is employed in numerical simulation to verify the combined procedure. The work is concluded in Section 4.

2 Combined shape control procedure

As for cable mesh reflector antennas, which consist of surface cables, rear cables, tie cables, ring truss and reflecting mesh (Thomson 2002), surface distortion usually exists due to thermal effect and manufacturing tolerance. By altering dimensions of some special cables, such as surface cables, tie cables, the distorted surface can be adjusted and its electromagnetic performance will be improved with reducing surface accuracy. The shape control algorithms

from simple structural disciplinary and structural electromagnetic multidisciplinary have already been investigated by Hafkta and Adelman (1985) and Padula et al. (1989), respectively. As for the integrated structural electromagnetic shape control concept presented by Padula et al. (1989), the surface rms accuracy added as a constraint in optimization model could promote optimization iterations and provide an efficient way of leading to faster convergence. This study proposes another way with optimality criterion to promote the convergence. As for antenna designers, the best far field electromagnetic performance of a reflector will be obtained when its surface approaches its nominal ideal state, or even exactly the nominal ideal state for solid smooth reflectors. The optimality criterion is here defined as the difference between the distorted shape and the nominal ideal state.

Supposing that the column vector of surface nodal coordinates in nominal ideal state is labeled as $\boldsymbol{r}^{(s)}$ and in any ith iteration state is labeled as $\boldsymbol{r}^{(i)}$, the surface nodal displacement vector which should be designed to drive the distorted surface towards the nominal ideal state in ith iteration is

$$\Delta \boldsymbol{r}^{(s,i)} = \boldsymbol{r}^{(s)} - \boldsymbol{r}^{(i)} \tag{1}$$

where $\Delta \boldsymbol{r}^{(s,i)}$ denotes the surface nodal displacement vector between the nominal ideal state and the ith iteration.

As for cable mesh reflector antennas, the surface nodal displacement vector between any two iterations can be expressed as a function of adjustable cable length variations with a coefficient sensitivity matrix

$$\Delta \boldsymbol{r} = \boldsymbol{K}_{te} \Delta \boldsymbol{l} \tag{2}$$

where $\boldsymbol{K}_{te}$ is the coefficient sensitivity matrix of surface nodal displacements with respect to cable member dimensions derived by Du et al. (2013), $\Delta \boldsymbol{l}$ is the column vector of adjustable cable length variations.

The optimality criterion is employed to drive the distorted surface towards the nominal ideal state to obtain better electromagnetic performance, thus the nodal displacement vectors in (1) and (2) are pre-designed to be equal. The expression in (2) is rewritten as

$$\Delta \boldsymbol{r}^{(s,i)} = \boldsymbol{K}_{te}^{(i)} \Delta \boldsymbol{l}^{(s,i)} \tag{3}$$

where $\Delta \boldsymbol{l}^{(s,i)}$ is the column vector of pre-designed adjustable cable length variations between the nominal ideal state and the ith iteration, $\boldsymbol{K}_{te}^{(i)}$ is the coefficient sensitivity matrix in the ith iteration.

Tanaka and Natori (2004, 2006) provided a measure of pseudo inverse of sensitivity matrix of surface nodal displacements with respect to cable tensions or cable force densities in shape control. In this study, the cable dimensions are directly determined through altering some adjustable cable dimensions not as cable tensions in Tanaka and Natori (2004,
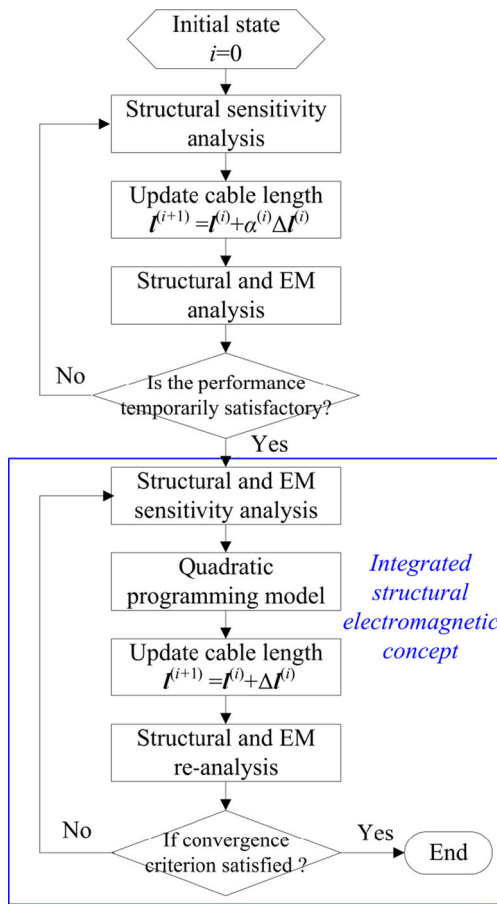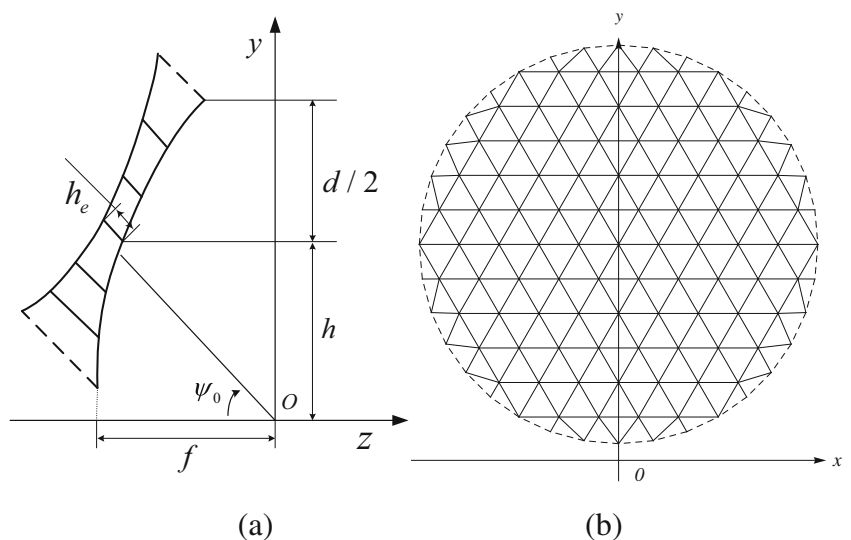
Fig. 1 Flow-chart of the combined shape control procedure

2006). The column vector of pre-designed adjustable cable length variations in (3) is expressed as

$$\Delta l^{(s,i)} = \left(K_{te}^{(i)} \right)^+ \Delta r^{(s,i)} \tag{4}$$

where the superscript operator '+' denotes the pseudo inverse operation.

The cable length vector in the next iteration will be written as

$$l^{(i+1)} = l^{(i)} + \alpha^{(i)} \Delta l^{(s,i)} \tag{5}$$

where $l^{(i)}$ represents the column vector of cable dimensions in ith iteration, and $\alpha^{(i)}$ is a step length in ith iteration.

The step length can be determined though the following one-dimensional optimization

$$
\begin{aligned}
&\text{find} && \alpha \\
&\text{min} && \varepsilon_{rms} \quad \text{or} \quad -D \\
&\text{s.t.} && \underline{T} \le T_i \le \overline{T}
\end{aligned}
\tag{6}
$$

where ε_{rms} denotes the surface accuracy between the nominal ideal state and present state, D is the boresight directivity. For small amount of distortion the antenna boresight directivity is consistent with surface accuracy. T_i is the ith cable tension, $\underline{T}$ and $\overline{T}$ are the lower and upper limits of cable tensions, respectively. Other constraints can also be added in this model according to design requirements.

When the surface accuracy in (6) decreases down or the boresight directivity in (6) increases up to a temporarily acceptable level, the integrated structural electromagnetic concept will be employed in the following implementation, which directly chooses electromagnetic performance - boresight directivity as object in optimization model. The following multidisciplinary implementation is the same as the authors' previous work in Zhang et al. (2015) by iteratively solving a sequential quadratic programming optimization model with gradient vector and Hessian matrix of boresight directivity with respect to cable member dimensions. The quadratic

Fig. 2 Geometry of an offset cable mesh reflector antenna in the nominal state, **a** *yoz* plane, **b** the aperture plane

(a)   (b)

Table 1 Parameters for cable mesh reflector in numerical example

reflector	Offset parabola $d = 9.23$ m, $f = 6$ m, $h = 5$ m
feed	Frequency 2 GHz Cosine-Q feed($Q_x = Q_y = 8.338$), y-polarized Feed tilt angle $\psi_0 = 41.64°$
cables	Min distance between two cables, $h_e = 0.2$ m triangular facets, 5 segments in radius Young's modulus $E = 20$ GPa cross-sectional area $A = 3.14$ mm^2

Table 2 Major parameters of far field patterns

	Max Directivity (dB)	HPBW (degree)	Sidelobe Level (dB)	
			Left	Right
Undistorted	43.364	1.261	−28.97	−28.97
Combined	43.363	1.261	−28.94	−29.18
ISE (Zhang et al. 2015)	43.363	1.261	−28.72	−29.38

programming optimization model can be expressed as (Zhang et al. 2015)

$$
\begin{aligned}
\text{find} \quad & \Delta l \\
\text{min} \quad & -D_0 - \mathbf{G}_D^T \cdot \Delta l - \frac{1}{2}(\Delta l)^T \mathbf{H} \Delta l \\
\text{s.t.} \quad & \mathbf{g}(l) = \mathbf{g}_0 + \mathbf{G}_g^T \cdot \Delta l \le \mathbf{0}
\end{aligned}
\tag{7}
$$

where D_0 is the boresight directivity in the nominal state, $\mathbf{G}_D$ is the gradient vector of boresight directivity with respect to cable length dimensions, $\mathbf{H}$ is the Hessian matrix of boresight directivity with respect to cable length dimensions, $\mathbf{g}_0$ is the constraints vector in the nominal state, and $\mathbf{G}_g$ is the gradient matrix of constraints with respect to cable length dimensions. The gradient vectors and Hessian matrix are updated during the iterations. The derivation of $\mathbf{G}_D$, $\mathbf{G}_g$ and $\mathbf{H}$ is based on two sensitivities (Zhang et al. 2015) - one is the electromagnetic sensitivity of boresight directivity with respect to surface nodal displacements, the other is the structural sensitivity of surface nodal displacements with respect to cable length dimensions.
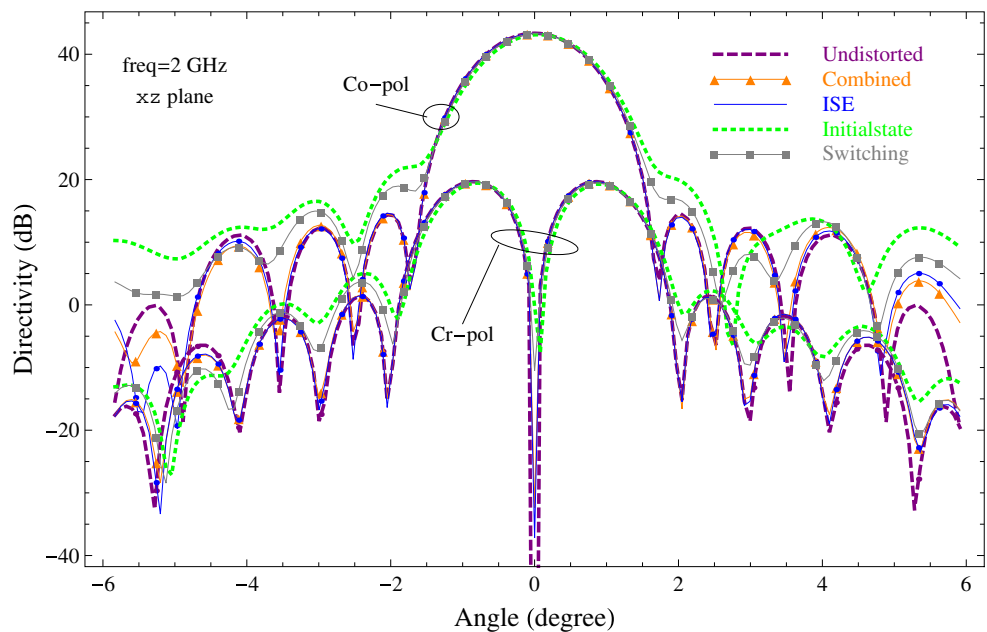
The column vector of adjustable cable length dimensions is updated by adding the solution of quadratic programming optimization model to their previous values

$$
l^{(i+1)} = l^{(i)} + \Delta l^{(i)}
\tag{8}
$$

where $\Delta l^{(i)}$ is the column vector of adjustable cable length variations by solving the multidisciplinary optimization model in ith iteration. When the boresight directivity increases up to a satisfactory value with convergence criterion, the combined procedure will stop and the optimal design will be obtained.

The main steps of this combined shape control procedure can be classified into two parts - one is the structural sensitivity analysis and pseudo inverse operation based on optimality criterion and the other is the implementation of integrated structural electromagnetic concept which directly chooses
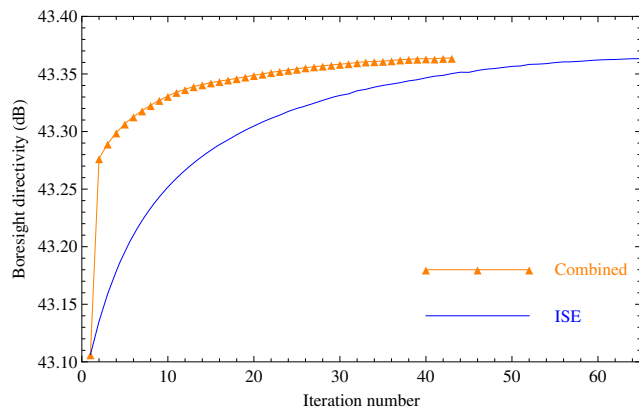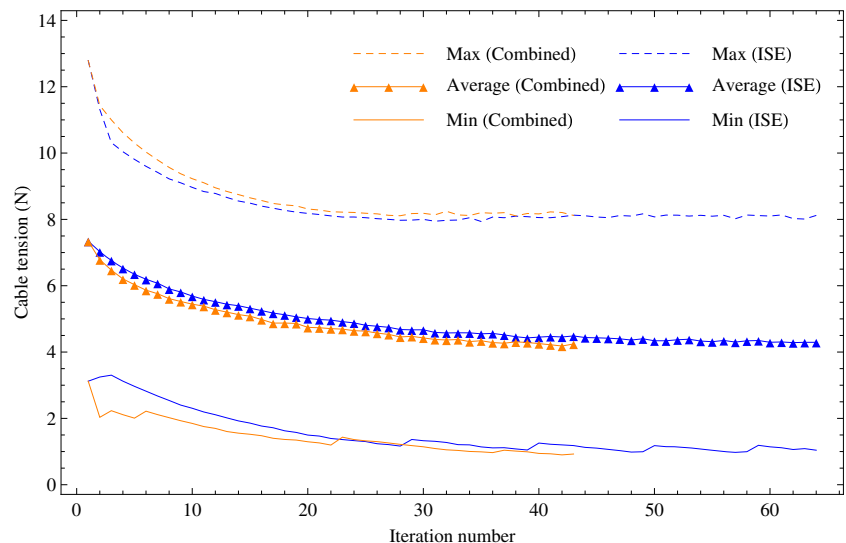
Fig. 3 Comparative results of far field patterns

Fig. 4 Iteration history of boresight directivity

Step 8: Update the cable length vector;
Step 9: Perform structural and electromagnetic re-analysis;
Step 10: Does the boresight directivity satisfy the convergence criterion? If no, go to Step 6, otherwise, export the optimum design.

It should be mentioned that the implementation from Step 6 to Step 10 belongs to the integrated structural electromagnetic concept which is referred to Zhang et al. (2015).

3 Example

To verify the performance of this combined shape control algorithm, an offset cable mesh reflector antenna is numerically analyzed. Figure 2 shows its geometry, where aperture diameter $d = 9.23$ m, focal length $f = 6$ m, offset height $h = 5$ m, feed tilt angle $\psi_0 = 41.64°$, the minimum distance between the surface and rear cables $h_e = 0.2$ m, and the aperture radius is divided into 5 segments to form triangular facets. These parameters are the same as the ones used previously by Zhang et al. (2015). In this simulation, the mesh surface divided into triangular elements by cables is treated by approximating it as a flat plane without considering the pillow effect (Meguro et al. 2003). A Cosine-Q feed with $Q_x = Q_y = 8.338$ is located at the focal point to radiate a y-polarized wave. The working frequency is set to be 2 GHz. The Young's modulus of cables is $E = 20$ GPa, and the cable cross-sectional area is $A = 3.14$ mm^2. Table 1 summarizes the parameters in this numerical example.

In order to show the effectiveness of this combined shape control procedure, the same distorted initial state in Zhang et al. (2015) is employed in this simulation. The initial distorted state was obtained by introducing some random

boresight directivity as object. The process of combined shape control procedure is shown in Fig. 1. Its main steps are as follows:

Step 1: Provide the initial state of a reflector and obtain its structural and electromagnetic performance, $i = 0$;
Step 2: Perform structural sensitivity analysis, and the pseudo inverse operation;
Step 3: Update the cable length vector with a step length optimization;
Step 4: Obtain the structural and electromagnetic (EM) performance;
Step 5: Does the surface accuracy decrease down or the boresight directivity increase up to a temporarily acceptable level? If yes, go on to Step 6, otherwise, go to Step 2;
Step 6: Perform structural and electromagnetic sensitivity analysis;
Step 7: Solve the multidisciplinary quadratic programming optimization model;

Fig. 5 Iteration history of tie cable tensions

errors into the cable dimensions and nodal positions. These random errors were assumed to be within 1 % of the nominal values to simulate manufacturing tolerance in the design process. The structural sensitivity analysis and pseudo inverse operation based on the optimality criterion are performed in the beginning. When the boresight directivity increases up to the value of 43.26 dB (D_0-0.1), the integrated structural electromagnetic concept will be employed in the following implementation. It should be mentioned that the undistorted state includes the inevitable systematic error from the faceting and D_0 represents the boresight directivity in the undistorted state of this mesh reflector. The convergence criterion of integrated procedure is also set to be $10\lg D^{(i+1)}$-$10\lg D^{(i)} \leq 10^{-4}$ same as that in Zhang et al. (2015). The tie cables are chosen as design variables to adjust the distorted surface in order to obtain a maximum directivity.

The far field patterns of the offset cable mesh reflector antenna are plotted in Fig. 3, where the purple dashed line represents the pattern in undistorted nominal state, the orange triangle marked line illustrates the optimal pattern by this combined procedure, the blue solid line represents the optimal pattern by integrated structural electromagnetic (ISE) procedure in Zhang et al. (2015), the green dotted line shows the pattern in distorted initial state, and the gray square marked line denotes the pattern at the switching point (after the first iteration) in this combined procedure. The major parameters of far field patterns including maximum directivity, half power beam width (HPBW), and sidelobe level are shown in Table 2. It can be concluded that the combined procedure shows nearly same electromagnetic performance with the integrated structural electromagnetic shape control. The iteration history of boresight directivity is shown in Fig. 4, where the combined procedure costs a less iteration number (43) than that of the integrated structural electromagnetic procedure (64). Furthermore, the boresight directivity increased up to 43.277 dB at the switching point in this combined procedure, which fulfilled the temporarily acceptable level (43.26 dB). The structural sensitivity analysis and pseudo inverse operation based on optimality criterion were implemented just once in the combined procedure. The effectiveness of this combined procedure is shown from the comparative results. It is due to the fact that the optimality criterion provides another efficient way of leading to faster convergence similarly as the surface accuracy constraint in Padula et al. (1989). The results demonstrate that the combined shape control algorithm which incorporates an optimality criterion can provide good electromagnetic performance with faster convergence.

The iteration history of maximum, average and minimum values of tie cable tensions for the combined procedure and integrated structural electromagnetic concept is shown in Fig. 5, where the dashed line represents the maximum values, triangle marked line denotes the average values, the solid line shows the minimum values, and orange is for the combined procedure, blue for the integrated procedure (ISE). The maximum, average, and minimum values of tie cable tensions in the optimal results of combined procedure are 8.0 N, 4.2 N, and 0.9 N, respectively.

4 Conclusions

A combined shape control procedure with optimality criterion and the integrated structural electromagnetic concept was developed for cable mesh reflector antennas. The optimality criterion was implemented by pseudo inverse of sensitivity matrix of surface nodal displacements with respect to cable member dimensions to drive the distorted surface towards the ideal shape. The combined shape control was applied to a distorted offset cable mesh reflector antenna, and the results demonstrated that the combined shape control could provide good electromagnetic performance with faster convergence.

References

Adelman HM, Padula SL (1986) Integrated thermal–structural–electro-magnetic design optimization of large space antenna reflectors. NASA TM-87713

Chen S, Ye S (1986) A guide-weight criterion method for the optimal design of antenna structures. Eng Optim 10:129–216

Du J, Zong Y, Bao H (2013) Shape adjustment of cable mesh antennas using sequential quadratic programming. Aerosp Sci Technol 30(1):26–33

Hafkta RT, Adelman HM (1985) R1 analytical investigation of shape control of large space structures by applied temperatures. AIAA J 23(3):450–457

Haftka RT (1991) Limits on static shape control for space structures. AIAA J 29(11):1945–1950

Haftka RT, Adelman HM (1985) R2 selection of actuator locations for static shape control of large space structures by heuristic integer programming. Comput Struct 20(1–3):575–582

Haftka RT, Adelman HM (1987) Effect of sensor and actuator errors on static shape control for large space structures. AIAA J 25(1):134–138

Hill J, Wang KW, Fang H (2013) Advances of surface control methodologies for flexible space reflectors. J Spacecr Rocket 50(4):816–828

Hoferer RA, Rahmat-Samii Y (2002) Subreflector shaping for antenna distortion compensation: an efficient fourier-Jacobi expansion with GO/PO analysis. IEEE Trans Antennas Propag 50(12):1676–1687

Jenkins CH, Kalanovic VD, Padmanabhan K, Faisal SM (1999) Intelligent shape control for precision membrane antenna and reflectors in space. Smart Mater Struct 8:857–867

Liu JS, Hollaway L (1998) Integrated structure-electromagnetic optimization of large reflector antenna systems. Struct Optim 16(1):29–36

Meguro A, Harada S, Watanabe M (2003) Key technologies for high-accuracy large mesh antenna reflectors. Acta Astronaut 53:899–908

Mitsugi J, Miura K, Yasaka T (1990) Shape control of the truss antenna. AIAA J 28(2):316–322

Miura A, Rahmat-Samii Y (2007) Spaceborne mesh reflector antennas using complex weaves: extended PO/periodic-MoM analysis. IEEE Trans Antennas Propag 55(4):1022–1029

Padula SL, Adelman HM, Bailey MC, Haftka RT (1989) Integrated structural electromagnetic shape control of large space antenna reflectors. AIAA J 27(6):814–819

Shimizu M (1996) Study of shape control for modular mesh antenna. Electron Commun 79(12):75–83, in Japan Part 1

Tabata M, Yamamoto K, Inoue T, Noda T, Miura K (1992) Shape adjustment of a flexible space antenna reflector. J Intell Mater Syst Struct 3(4):646–658

Tanaka H, Natori MC (2004) Shape control of space antennas consisting of cable networks. Acta Astronaut 55:519–527

Tanaka H, Natori MC (2006) Shape control of cable-network structures based on concept of self-equilibrated stresses. JSME Int J Ser C 49(4):1067–1072

Thomson MW (2002) AstroMesh^{TM} deployable reflectors for Ku- and Ka-band commercial satellites. 20th AIAA Int. Communication Satellite Systems Conf. and Exhibit, Quebec, Canada, May 2002: 1–9

Tolson RH, Huang JK (1992) Integrated control of thermally distorted large space antennas. J Guid Control Dyn 15(3):605–614

Zhang S, Du J, Duan B, Yang G, Ma Y (2015) Integrated structural-electromagnetic shape control of cable mesh reflector antennas. AIAA J 53(5):1395–1398